Two-Electron Correlations in $e+H \rightarrow e+e+p$ Near Threshold

Daiji Kato* and Shinichi Watanabe†

Department of Applied Physics and Chemistry, University of Electro-Communications, 1-5-1, Chofu-ga-oka, Chofu-shi, Tokyo 182, Japan

(Received 6 September 1994)

We present an *ab initio* calculation of the ionization cross section of atomic hydrogen near threshold with precision that compares excellently with the Shah-Elliot-Gilbody experiment [J. Phys. B **20**, 3501 (1987)]. This fills the gap between theory and experiment down to 0.1 a.u. above threshold, complementing the recent spectacular work of Bray and Stelbovics [Phys. Rev. Lett. **70**, 746 (1993)]. The angular momentum distributions of the secondary electron display an evolution in correlation patterns toward the threshold.

PACS numbers: 34.50.Fa, 34.80.Dp

Electron-impact ionization of hydrogen is one of the most fundamental processes involving one heavy and two light particles in disintegration without charge transfer. Its particular simplicity allows one to estimate the order of magnitude of the total cross section readily [1]. Nonetheless, theory has been considered largely incomplete because theoretical methods [2,3] could evaluate cross sections with a far less precision than can the experiment [4]. A terse historical account of this can be found in the recent Letter by Bray and Stelbovics that has succeeded in bridging this long-standing gap from intermediate to high energies by means of the convergent close-coupling (CCC) method [5]. However, they left a gap on the low-energy side unresolved. The current techniques are well suited to the study of threshold ionization whereas the CCC method is not, though an enlargement of the basis set might as well improve the convergence of the CCC method even at low energies. The present work investigates the low-energy region rather close to threshold within the framework of the time-independent scattering theory. Throughout this Letter, we use atomic units, i.e., 1 a.u. of length $\approx 5.29 \times 10^{-11}$ m (Bohr radius a_0) and 1 a.u. of energy ≈ 27.2 eV.

For clarifying the spirit, let us employ an index $\kappa = 1/\sqrt{2|E|}$, an analog of the single-electron wavelength, for both below and above threshold. Here and throughout, E is measured from the threshold so that κ represents the distance in energy from the threshold and serves as a rough measure of the spatial range where the two-electron correlation [6] is important; the characteristic distance associated with the correlation is of the order of κ^2 according to Wannier [7]. The energy range may be divided into three regions. The high-energy region ($\kappa \ll 1$) is where the perturbative treatment yields moderately reliable results. As a matter of fact, the controversial ratio of the single-to-double ionization of He by photon impact at $\kappa \ll 1$ appears to be reasonably well represented by perturbation theory [8]. Here, the electron-electron correlations occur at rather short mutual distances during a short time interval, thus the two electrons may be considered largely independent. The low-energy region ($\kappa \geq 1$) is, on the contrary, where the correlations become particularly important because the incident electron has ample time to see the detailed level structure of the target atom; the target in turn has ample time to respond to the electric field exerted by the incident electron. Here, the distortion of the two-electron wave function reaches such a degree that the mixing of a large number of configurations is needed, and a nonperturbative scheme must be employed. The intermediate-energy region ($\kappa \sim 1$) contributes to the major portion of the energy-integrated cross section. Regarding this region by including a number of configurations allows an improvement over perturbation theory [5]. The interest of the present work is in the moderately low positive-energy region where $\kappa \sim 3$ and where achieving convergence by configuration mixing using a separable basis set shows a sign of difficulties. Ironically, the cross section in this low-energy region is very small, making it particularly difficult to evaluate the most interesting physical quantities such as the threshold exponent, because they are influenced by the long range correlations. In this regard, the situation is analogous to second order phase transitions; there the correlation length diverges toward the critical point. The numerical determination of the critical exponents requires to encasing an ever larger volume.

Another facet of the ionization near threshold is our unsatisfactory understanding of the quantum-classical correspondence in the two-electron atom. It has not been long since the comprehensive picture of doubly excited states emerged from the molecular classification of angular correlations [9,10] combined with Lin's nomenclature of the radial correlation patterns [11]. Surprisingly, the moleculelike level patterns persist even up to $\kappa \sim 6$ in both He [12] and H^- [13], whereas the recent rejuvenation of the classical dynamics study and semiclassical quantization [14,15] anticipates occurrences of irregularity due to instability. Because Wannier's threshold law [7] for the total ionization cross section was first derived on the basis of the dynamical instability of a particular

 © 1995 The American Physical Society

class of trajectories that travel astride the potential ridge at $\vec{r}_1 = -\vec{r}_2$, the regularity of the quantum spectra slightly below threshold is an apparent mystery [16]. Examining the quantum mechanics of the near-ionization region is extremely intriguing from this viewpoint.

As mentioned earlier, in representing the ionization process near threshold we need good basis functions adaptive to various distortions caused by strong correlations. For this precise reason, we employed the hyperspherical close-coupling (HSCC) method in our preliminary work for ionization [17], using the Poet-Temkin (PT) s-wave model [18] in which the angular momenta of both electrons are limited to 0, namely the s^2 configuration. The hyperspherical coordinates make the two-electron atomic Schrödinger equation locally quasiseparable,

$$H = -\frac{1}{2}\vec{\nabla}_1^2 - \frac{1}{2}\vec{\nabla}_2^2 - \frac{1}{r_1} - \frac{1}{r_2} + \frac{1}{|\vec{r}_1 - \vec{r}_2|} \rightarrow -\frac{1}{2}\frac{d^2}{dR^2} + \frac{\mathcal{H}_{\text{adia}}(R;\Omega)}{2R^2}, \quad (1)$$

where the local adiabatic Hamiltonian $\mathcal{H}_{\text{adia}}$ depends on the hyperradius $R = \sqrt{r_1^2 + r_2^2}$ only parametrically, and $\Omega = \{\alpha = \arctan(r_1/r_2), \hat{r}_1, \hat{r}_2\}$ represents the rest of the coordinates symbolically. The symbol $\rightarrow$ is employed here to note the rescaling of the wave function Ψ to $R^{5/2}\cos\alpha\sin\alpha\Psi$. The HSCC method exploits basis functions $\{\Phi_\mu(R;\Omega)\}$ that are defined by the adiabatic eigenvalue problem,

$$\mathcal{H}_{\text{adia}}\Phi_\mu(R;\Omega) = U_\mu(R)\Phi_\mu(R;\Omega), \quad (2)$$

so that the basis set is adiabatically optimized to the local potential field and forms a complete orthonormal set. The method then expands the solutions of the two-electron atomic Schrödinger equation in a piecewise diabatic way, namely,

$$\Psi_n(\vec{r}_1,\vec{r}_2) = \sum_\nu F_{n\nu}(R)\Phi_\nu(R_i;\Omega), \quad (3)$$

where the index n labels the solution and $R \in [R_i - h, R_i + h]$ for some reasonably chosen values of R_i and h. The coefficients $F_{n\nu}(R)$ satisfy a set of coupled ordinary differential equations in the form of standard close-coupling equations amenable to various numerical schemes. A strength of the HSCC method is that even an expansion over a moderate number of channel functions yields well-converged solutions in the interval $R \in [0, R_m]$ where the upper radius R_m is finite. This is convincingly demonstrated by Tang *et al.* [12] in the case of photoionization of He. However, one fundamental problem with the method is that the adiabatic basis functions do not correspond to the three disintegrated particles even in the asymptotic region where R goes to infinity. Thus, in Ref. [17], we extracted the ionization amplitude by projecting the internal HSCC solutions onto the asymptotic solutions represented in the independent particle coordinates. Here, we introduce a new version of projection which turns out to be simpler and more convergent [19].

Regarding the asymptotic region, we need to recall that unlike the two-body problem there exists no analytically expressible asymptotic solution that can cover every possible configuration, namely, $(r_1 \rightarrow \infty, r_2 < \infty)$, $(r_1 < \infty, r_2 \rightarrow \infty)$, and $(r_1 \rightarrow \infty, r_2 \rightarrow \infty)$. Only for the first two configurations approximate solutions are known [20]. This fact articulates an inherent difficulty of the three-body disintegration problem. Nonetheless, what is required of the asymptotic solutions is to represent the incoming-wave boundary condition as well as to normalize the ionization flux. The former is straightforward while the latter at first appears to require *a priori* knowledge of some analytical asymptotic solutions. However, we can argue such a concern away as follows. Suppose we enclose the internal region with a large enough box defined by a hypersphere of radius $R = R_m$ so as to contain all the dynamical information therein. At $R > R_m$ the asymptotic solutions are represented by the linear combination with the following delimited solutions in which the effect beyond the monopole term of the electron-electron interaction is presumed negligible,

$$\Theta^{\pm}_{\epsilon l_1 l_2}(\vec{r}_1,\vec{r}_2) = f^{\pm}_{kl_1}(r_1)\phi_{\epsilon l_2}(r_2)Y_{l_1 l_2 LM}(\hat{r}_1,\hat{r}_2) \qquad (r_1 \geq r_2), \quad (4)$$

where $f^{\pm}_{kl}$ pertain to the outgoing and incoming spherical waves. We note that on account of the obvious symmetry of the problem, we limit our subsequent considerations to the domain $r_1 \geq r_2$. Here, $\phi_{\epsilon l_2}(r_2)$ represents the target state and satisfies the Coulomb Schrödinger equation with the boundary condition at $r_2 = r_m = R_m/\sqrt{2}$, $(\partial/\partial r_2 - b/r_2)\phi_{\epsilon l_2}|_{r_2=r_m} = 0$, where b is an arbitrary constant whose specific value is irrelevant to the physical observables provided r_m is taken sufficiently large. As a result of this boundary condition, the continuum energy spectrum of the target states is inevitably discretized. Then we exclude the region where r_2 is greater than r_m. This does not mean that the excluded region is entirely out of our consideration. It would mean, instead, we constructed wave packets by integrating over discretized energy (or momentum) intervals so that the wave packets localized near the proton are formed. Consequently, the scheme is able to resolve details in energy as well as in momentum domains that are no finer than the discretized energy as well as momentum intervals.

Now, the internal and asymptotic solutions are matched across the arc defined by $R = R_m$, demanding the equality of the logarithmic derivative so that the linear combination coefficients of the delimited solutions are uniquely determined. From these coefficients the S matrix $S_{\epsilon' l_1' l_2', \epsilon l_1 l_2}(E)$, where ϵ and ϵ' pertain to the energy index of the target state, is algebraically calculated. The

solution has the asymptotic form

$$\Theta^{-}_{\epsilon l_1 l_2}(\vec{r}_1,\vec{r}_2) + \sum_{l_1',l_2'} \int_{\epsilon'} \Theta^{+}_{\epsilon' l_1' l_2'}(\vec{r}_1,\vec{r}_2) S_{\epsilon' l_1' l_2',\epsilon l_1 l_2}(E) . \quad (5)$$

Once the S matrix is obtained, the total cross section, energy-differential cross section, etc. follow readily from standard formulas with the understanding that we replace the integration with respect to ϵ by the summation with the appropriate quadrature weights.

Let us move on to the demonstration. First, taking the PT model as an example, we show that our method achieves an excellent convergence over a wide energy range. Figure 1 shows the model total ionization cross section versus energy on a log-log scale calculated with 60 channels, and R_m was varied between 50 and 200 a.u. till convergence was achieved within a few %. This result *confirms* the convergence of the calculation by Bray and Stelbovics (cf. Fig. 1 in Ref. [21]). Stated differently, this model calculation suggests that for a given angular configuration defined by a specific pair of angular momenta (l_1, l_2), the HSCC method can represent the radial degrees of freedom very well over a wide energy range. Next, we focus our attention on projectile energies from 0.5 to 0.9 a.u., i.e., $E = 0$–0.4 a.u. We show in Fig. 2 the total ionization cross section σ of the real process $e + \mathrm{H}(1s) \rightarrow e + e + p$ as well as σ/E which is a more sensitive function of correlations. The number of channels employed for expansion is listed in Table I, and the matching radius R_m was varied between 100 and 200 a.u. The result is compared with that of Bray and Stelbovics [5] and that of Callaway [3] as well as to the Shah-Elliot-Gilbody experiment [4]. The relative difference in σ between our result and the experiment is within a few % from $E = 0.1$ to 0.4 a.u. However, as the energy gets closer to threshold ($E < 0.1$ a.u.), the largest difference reaches 20%. The difference in σ may be traced, on

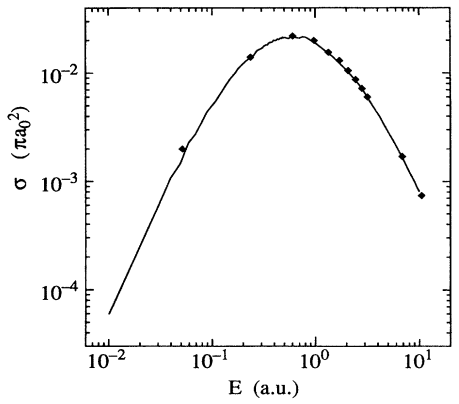

FIG. 1. Total ionization cross section (σ) of hydrogen using the Poet-Temkin model [$(s^2)^1S^e$]. Solid line represents present work, and filled diamonds represent the convergent close-coupling method [21].

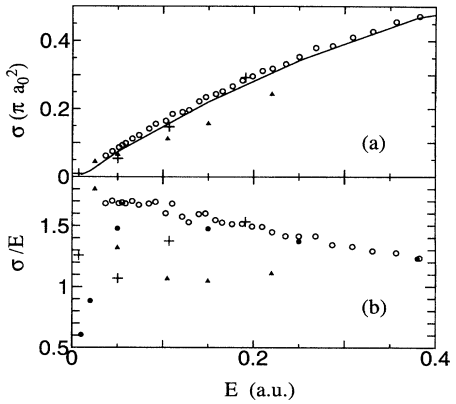

FIG. 2. (a) Total ionization cross sections of the real process versus energy. Solid line represents present work, open circles experimental data from [4], crosses the convergent close-coupling method (private communication [5]), and filled triangles the pseudostate expansion method [3]. (b) σ/E, a function that reveals the details near threshold. Filled circles represent present work, and the other symbols are as in (a).

the one hand, to the experimental difficulty of measuring slow electrons, and, on the other hand, to the theoretical difficulty of resolving the details of the continuum states which are represented by discretization; the states so discretized at a fixed R_m get too coarse to resolve the cross section as $E \rightarrow 0$. As for the function σ/E, our result is smooth whereas the CCC result of Bray and Stelbovics shows a noticeable fluctuation. Note, however, the rapid decline toward threshold in our result reflects merely the matching at a finite R_m to the approximate asymptotic solutions. That is, it is not an indication of Wannier's threshold behavior. Figure 3 shows the angular momentum distributions of the secondary electron [l_2 in Eq. (4)] at $E = 0.97$, 0.419, and 0.0515 a.u. One notices that the transition is more dipolelike ($\Delta l_2 = 1$) at higher energies which complies with our understanding. The distribution does smear out toward the threshold though the dominance of the dipole transition maintains even at the lowest energy we examined. Should its dominance be completely smeared out at even lower energies? What will happen to this angular momentum distribution when the Wannier threshold law sets in? We leave these questions for future investigations.

Wannier's threshold law $\sigma \propto E^{1.127}$ [7] has not been demonstrated by any fully quantum mechanical treatment. Going closer to threshold so as to examine the cusp of the

TABLE I. List of $\mu_{\max}$, the maximum number of channels coupled. Regarding the labeling of states, $^3S^e$ means, for example, that total orbital angular momentum $L = 0$, total spin $S = 1$, and the parity is even.

	$^{1,3}S^e$	$^{1,3}P^o$	$^{1,3}D^e$	$^{1,3}F^o$	$^{1,3}G^e$	$^{1,3}H^o$	$^{1,3}I^e$
$\mu_{\max}$	95	154	188	187	166	181	194

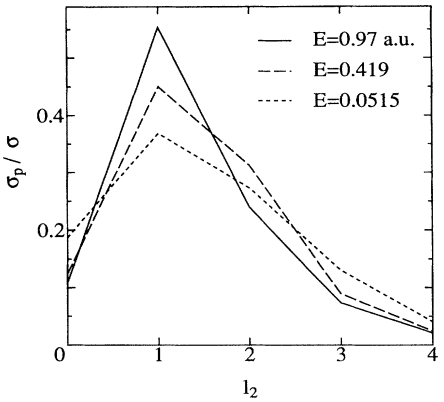

FIG. 3. The angular momentum distributions of the secondary electron (σ_p/σ) at $E = 0.97$, 0.419, and 0.0515 a.u., where σ_p represents partial ionization cross section.

Cvejanović-Read experiment [22] would require one to extend R_m to thousands of atomic units [23]. Sustaining a numerical stability to such a distance is beyond the scope of any *ab initio* theoretical method to date. However, our method is promising because of its unbiased radial basis functions.

To conclude, we have succeeded in evaluating the low-energy ionization cross section with a precision comparable to that of the Shah-Elliot-Gilbody experiment down to ~0.1 a.u. Even at these energies, the angular momentum distributions of the secondary electron have shown the dominance of the dipole transition. The adiabatic basis functions adaptive to strong correlations should become progressively important for exploring even lower energy regions.

We thank Dr. I. Bray for generously providing us with his data and Dr. M. Matsuzawa for useful advice and encouragement. We appreciate discussions with Dr. C. D. Lin and Dr. C. H. Greene made possible by a U.S./Japan collaborative program sponsored by the Japan Society for the Promotion of Science. D. K. acknowledges gratefully the fellowship provided by the same organization. And S. W. acknowledges a partial support by a Grant-in-Aid for Scientific Research on Priority Area "Atomic Physics of Highly Charged Ions" from the Ministry of Education, Science and Culture of Japan.

*Electronic address: kato@power1.pc.uec.ac.jp
†Electronic address: shin@power1.pc.uec.ac.jp

[1] G. Peach, Proc. Phys. Soc. **87**, 381 (1969); (private communication).
[2] D. F. Gallaher, J. Phys. B **7**, 362 (1974); J. Callaway and D. H. Oza, Phys. Lett. **72A**, 207 (1979); T. T. Scholz, H. R. Walters, and P. G. Burke, J. Phys. B **23**, L467 (1990), and references therein.
[3] J. Callaway, Phys. Rev. A **44**, 2192 (1991).
[4] M. B. Shah, D. S. Elliot, and H. B. Gilbody, J. Phys. B **20**, 3501 (1987).
[5] I. Bray and A. T. Stelbovics, Phys. Rev. Lett. **70**, 746 (1993); At. Data Nucl. Data Tables **58**, 67 (1994); (private communication).
[6] The two-electron correlation has been only elusively defined as the difference between the exact and Hartree-Fock calculations. Here we interpret the correlation in a more mechanistic sense. It is the mechanism that helps the electrons maintain the unstable configuration $\vec{r}_1 = -\vec{r}_2$, where $\vec{r}_1$ and $\vec{r}_2$ are the position vectors of the two electrons from the nucleus, whereupon the electronic repulsion $1/r_{12}$ is minimized.
[7] G. Wannier, Phys. Rev. **90**, 817 (1953); A. R. P. Rau, Phys. Rev. A **4**, 207 (1971); R. Peterkop, J. Phys. B **4**, 513 (1971). See also Refs. [14] and [23].
[8] J. A. R. Samson, C. H. Greene, and R. J. Bartlett, Phys. Rev. Lett. **71**, 201 (1993); K. Hino, P. M. Bergstrom, Jr., and H. H. Macek, Phys. Rev. Lett. **72**, 1620 (1994), and references therein.
[9] M. E. Kellman and D. R. Herrick, J. Phys. B **11**, L755 (1978).
[10] H. J. Yuh, G. S. Ezra, P. Rehmus, and R. S. Berry, Phys. Rev. Lett. **47**, 497 (1981); J. E. Hunter and R. S. Berry, Phys. Rev. A **36**, 3042 (1987), and references therein.
[11] C. D. Lin, Adv. At. Mol. Phys. **22**, 77 (1986).
[12] J. Z. Tang, S. Watanabe, M. Matsuzawa, and C. D. Lin, Phys. Rev. Lett. **69**, 1633 (1992).
[13] J. Z. Tang and I. Shimamura, Phys. Rev. A **51**, 1738 (1995).
[14] S. Watanabe, Phys. Rev. A **36**, 1566 (1987).
[15] G. S. Ezra, K. Richter, G. Tanner, and D. Wintgen, J. Phys. B **24**, L413 (1991); J. Müller, J. Burgdörfer, and D. Noid, Phys. Rev. A **45**, 1471 (1992), and references therein.
[16] Overlapping of resonances belonging to two different shells has been recently observed in He [12]. There is no knowing at the moment what features the spectra will have when many shells begin to overlap.
[17] S. Watanabe, Y. Hosoda, and D. Kato, J. Phys. B **26**, L495 (1993).
[18] R. Poet, J. Phys. B **11**, 3081 (1978); A. Temkin, Phys. Rev. **126**, 130 (1962).
[19] This prescription has been independently found and recently applied to a molecular dissociation problem. See K. Nobusada, K. Sakimoto, and K. Onda, Chem. Phys. Lett. **216**, 613 (1993); K. Sakimoto and K. Onda, J. Chem. Phys. **100**, 1171 (1994).
[20] E. O. Alt and A. M. Mukhamedzhanov, Phys. Rev. A **47**, 2004 (1993).
[21] I. Bray and A. T. Stelbovics, Phys. Rev. Lett. **69**, 53 (1992).
[22] S. Cvejanović and F. H. Read, J. Phys. B **7**, 1841 (1974).
[23] A. K. Kazansky and V. N. Ostrovsky, J. Phys. B **25**, 2121 (1992).